Impact of the volume change on the ageing effects in Cu–Al–Ni martensite: experiment and theory

Impact of the volume change on the ageing effects in Cu–Al–Ni martensite: experiment and theory

Anna Kosogor[1]**, Dezhen Xue**[2]**, Yumei Zhou**[2]**, Xiangdong Ding**[2]**,**
Kazuhiro Otsuka[3]**, Victor A L'vov**[1,4]**, Jun Sun**[2] **and Xiaobing Ren**[2,3]

[1] Institute of Magnetism, 36-b Vernadsky Blvd, Kyiv 03142, Ukraine
[2] Multi-disciplinary Materials Research Center, Frontier Institute of Science and Technology,
State Key Laboratory for Mechanical Behavior of Materials, Xi'an Jiaotong University, Xi'an 710049,
People's Republic of China
[3] Ferroic Physics Group, National Institute for Materials Science, Tsukuba, 305-0047, Ibaraki, Japan
[4] Taras Shevchenko University, Glushkov str. 2, build.5, Kyiv 01601, Ukraine

E-mail: annakosogor@gmail.com and xuedezhen@gmail.com

Abstract
The time evolution of the physical properties of martensite during martensite ageing is
traditionally explained by the symmetry-conforming short-range order (SC-SRO) principle,
which requires the spatial configuration of crystal defects to follow the symmetry change of
the host lattice. In the present study, we show that the volume change of the host lattice also
contributes to the ageing effects in Cu–Al–Ni shape memory alloy besides the symmetry
change. To substantiate this statement the gradual increase of the storage modulus with time at
constant temperature was measured by dynamic mechanical analysis (DMA) and the
experimental results were quantitatively described in the framework of the
symmetry-conforming Landau theory of martensitic transformations in a crystal with defects.
The comparison of experimental and theoretical results confirmed that the time dependence of
the storage modulus is caused by two different physical mechanisms. Evaluations showing that
the first mechanism is driven by the spontaneous symmetry change and the second mechanism
is caused by the volume change after the martensitic transformation was carried out.

(Some figures may appear in colour only in the online journal)

1. Introduction

The drastic dependence of the elastic properties of crystalline solids on the type, concentration, spatial distribution and mobility of crystal defects is a matter of common knowledge. The defects distort the crystal lattice and induce mechanical stress, which may be referred to as 'internal stress', to emphasize that it can arise even in the absence of external forces applied on single- and polycrystalline specimens. The internal stress concept is useful for the description of different physical phenomena, such as the interaction of hydrogen atoms with the crystal lattice of metals [1], giant magnetically induced deformation of twinned ferromagnetic crystals [2–4]

and many others. The stresses produced by the crystal defects vary with time due to defect diffusion. As a rule, the characteristic time of diffusion noticeably exceeds the time of the elastic response of the solid to the externally applied force and, thus, the deformational and magnetic properties of the solid slowly evolve even under constant physical conditions (see e.g. [5, 6] and references therein). The physical effects caused by the evolution of the defect subsystem are especially pronounced in the shape memory alloys, because of the thermodynamic instability of their crystal lattice, which exhibits itself as a martensitic transformation (MT) of the thermoelastic type [7, 8]. The cooperative (experimental and theoretical) study of the unstable crystal lattice interacting

with the defect subsystem is a challenging scientific problem. This problem is of practical interest due to the numerous applications of shape memory alloys.

The MT of the shape memory alloy is a first-order phase transition from a high-symmetry (cubic) phase to a low-symmetry (tetragonal, rhombohedral, orthorhombic, etc) phase. The MT always involves symmetry breaking and a volume change. Long-term storage of the alloy in its martensitic state is accompanied by a gradual change of physical properties with time [9–16]. Such time-dependent behavior is known as martensite ageing. Since martensite ageing largely affects the reliability of shape memory devices, related studies are of practical importance.

Practically important manifestations of martensite ageing include the increase of reverse MT temperature (martensitic stabilization) [13, 16–18], the appearance of rubber-like behavior [9–11] and the noticeable increase of the elastic modulus [19] with ageing time. Several physical mechanisms have been proposed to explain martensite ageing, with most presuming that the property changes during martensite ageing are caused by a spatial reconfiguration of atoms during martensite ageing [20] and an appropriate reconfiguration of the crystal defect subsystem (see [21] and references therein). In the case of point defects, the reconfiguration process is governed by the symmetry-conforming short-range order (SC-SRO) principle [22, 23]. The main idea of this principle is that the spatial distribution of point defects in the aged alloy possesses the symmetry of the crystal lattice. After martensitic transformation, the crystal symmetry is broken. Consequently, according to this principle, the spatial distribution of point defects with high symmetry needs to adopt a lower symmetry after the MT. Thus the reconfiguration of point defects during martensite ageing is driven by the symmetry mismatch between the host crystal lattice and the spatial distribution of point defects.

To fully comprehend martensite ageing, one should take into account that the reconfiguration of point defects results in the appearance of slowly variable lattice distortion [24] and appropriate internal stress on the lattice [25, 26]. The internal stress concept enables the generalization of the SC-SRO principle [25, 26]: martensite ageing is accompanied by a slow reconfiguration of different mobile defects (point defects, dislocations, stacking faults, incoherent interfaces, etc) and this reconfiguration results in a slow increase of the absolute value of the martensitic transformation strain. The ageing process is accompanied by a decrease in the volume of the alloy specimen caused by the tendency towards close packing of atoms [25].

The MT is characterized mainly by shear deformation of the crystal lattice $|\varepsilon_M| \sim 1$–10%. The comparatively small volume change during MT ($|\Delta V/V| \sim 0.1$–1%) is often considered as a secondary effect, which can be disregarded when the basic characteristics of MTs and transformational properties of the shape memory alloys are analyzed. This view on the role of volume change of the shape memory alloy is called into question by both experimental studies and theoretical estimations. In particular, a hydrostatic pressure of about 1 GPa results in a small volume change but

a noticeable shift of the MT temperature [27, 28]; the volume magnetostriction of ferromagnetic Ni–Mn–Ga alloy ($\Delta V/V \sim -0.1$%) results in the appearance of a coupled magnetostructural transformation [29]. The significant role of the volume change was emphasized also by recent studies of the thermodynamic and elastic properties of shape memory alloys with defects [25, 26, 30]. It was shown that the volume change arising due to the defect reconfiguration noticeably changes the characteristic MT temperatures [25, 26] and storage elastic moduli [30] of the alloys.

The necessity for a careful consideration of the volume change of shape memory alloy can be illustrated by simple physical considerations. The volume change during MT results in an energy density change $|\Delta F_1| \sim |\Delta V/V|B \sim$ 0.1–1 GPa (where $B \sim 100$ GPa is the bulk elastic modulus). The spontaneous shear of the crystal lattice during MT results in an energy density change $|\Delta F_2| \sim |\varepsilon_M|C' \sim 0.1$–1 GPa (where $C' \sim 10$ GPa is a realistic value of the shear modulus of the shape memory alloy in the vicinity of the MT temperature, see below). The energy changes ΔF_1 and ΔF_2 are of the same order of magnitude; therefore, the volume change must be taken into account for a full comprehension of the transformational and elastic properties of shape memory alloys.

In the present study, the time evolution of the storage modulus of Cu–Al–Ni shape memory alloy was measured by dynamical mechanical analysis (DMA) at different temperatures. The experimental results were quantitatively described by the symmetry-conforming Landau theory [25, 26], taking into account both shear deformation and the volume change of the alloy with defects. Our results show that the accurate description of the influence of martensite ageing on storage modulus requires the consideration of both the symmetry change effect and the volume change effect. Our studies suggest that the spatial redistribution of crystal defects during martensite ageing is driven by both the spontaneous symmetry change and the volume change during MT.

2. Experimental details

We used Cu–13.8Al–4.0Ni polycrystalline alloys. Base ingots were made by melting 99.99% pure Cu, 99.99% pure Al and 99.9% pure Ni using an induction furnace with an Ar atmosphere. After homogenization at 1273 K for 24 h in the Ar atmosphere, specimens were cut into appropriate sizes for each measurement. They were solution-treated at 1273 K for 2 h in an Ar atmosphere, followed by quenching in water.

Martensite ageing effects on the dynamic properties (storage modulus and internal friction ($\tan\delta$)) were measured by DMA in a single cantilever mode. During the DMA measurement, the specimen was first cooled to the ageing temperature at a cooling rate of 2 K min^{-1} and then aged at this temperature. The dynamic properties as a function of ageing time were recorded after temperature stabilization. In order to erase the influence of the martensite ageing effect at the previous testing temperature on the results of the next testing temperature, we heated the specimen to a temperature of 500 K (far above the austenite finish
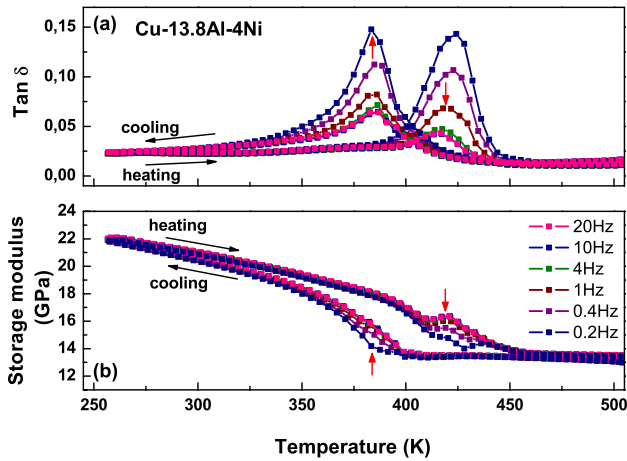
Figure 1. Martensitic transformation in Cu–13.8Al–4.0Ni alloy characterized by (a) internal friction and (b) storage modulus by dynamic mechanical analysis measurement.
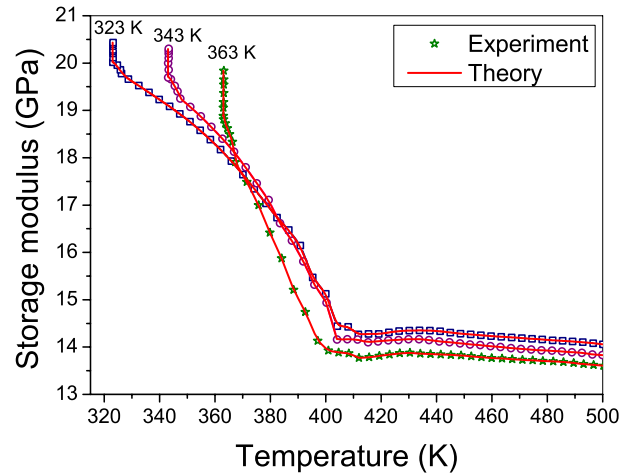

Figure 2. Experimental (points) and theoretical (lines) temperature dependences of the storage modulus when the Cu–13.8Al–4.0Ni alloy is cooled down to 363, 343 and 323 K and aged at these temperatures. The affect of ageing on the storage modulus is illustrated by the vertically arranged experimental points and vertical segments of the lines.
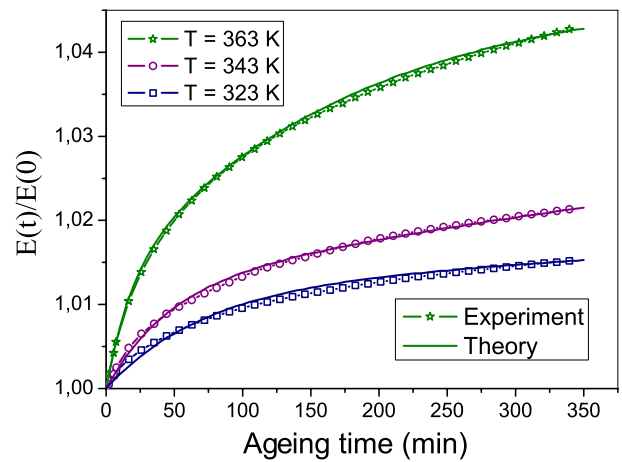

Figure 3. The experimental (points) and theoretical (lines) time dependences of the storage modulus of the specimen aged at different temperatures.

T_{AF} temperature) and maintained there for several minutes for each testing run. The Cu–13.8Al–4.0Ni alloy was aged at different temperatures (323/343/363 K) and different frequencies (0.2/0.4/1/4/10/20 Hz).

Figure 1 shows curves of the storage modulus and internal friction versus temperature upon cooling and heating under various frequencies. It is seen that the β_1 to γ_1 (cubic-to-orthorhombic) MT is characterized by a frequency-independent storage modulus dip and an internal friction peak, which result from the elastic softening and the hysteretic movement of both parent-martensite phase boundaries and twin boundaries under the ac external stress field during DMA measurement, respectively. The forward and reverse MT temperatures (the peak temperature of internal friction on cooling and heating) are about 385 K and 420 K, respectively.

The dotted points in figure 2 show the experimental values of storage modulus when the specimen was cooled to 323, 343, 363 K and then held (aged) at these temperatures for 6 h. The time dependences of storage modulus observed at these temperatures are illustrated in figure 3. The experimental results show that the higher the ageing temperature, the more pronounced is the variation of elastic modulus during martensite ageing. The solid curves in figures 2 and 3 are computed using the symmetry-conforming Landau theory, of which the details of computations are explained below.

3. Theoretical basis

A one-dimensional model for the description of martensite ageing effects was formulated in [31]. The model dealt with the martensitic structure formed by two variants of the martensitic phase. The transformational properties of this structure were described by two interrelated scalar parameters. The first one (referred to as 'strain') was considered proportional to the spontaneous deformation of the crystal lattice in the course of MT and the second one (called 'shift') characterized shuffling of the atomic layers. It was assumed that the strains immediately respond to the

mechanical load but the shuffles 'relax according to some slower kinetics' [31]. Only the second-order and bilinear terms in strain and shift components were included in the mathematical expression for the free energy. The basic points of the one-dimensional model were introduced later in the framework of Landau theory [32, 33] without the binding of the slowly relaxing parameter to the shuffle mechanism.

The one-dimensional model and its introduction in the framework of Landau theory provides the *qualitative* description of such effects of martensite ageing as the rubber-like behavior of shape memory alloys and martensite stabilization. However, this model cannot interrelate the martensite ageing effects with the strain tensor components, elastic moduli and volume change, because it neglects (a) the three-dimensional character of spontaneous deformation of alloy and correspondent symmetry change; (b) the third- and fourth-order terms of the equation for the free energy;

(c) the volume change that accompanies the martensitic transformation of the alloy. For this reason the time dependence of elastic moduli was not considered in [31–33]. Below we show that the experimental dependence of the storage elastic modulus on the ageing time can be explained only taking into account points (a)–(c).

In this section, we formulated the theoretical model for the ageing effect on the storage modulus, based on the symmetry-conforming Landau theory [25, 26]. The order parameters of the thermoelastic martensitic transformation are linear combinations of the strain tensor components. The diagonal and non-diagonal components form the order parameters of cubic–tetragonal and cubic–rhombohedral MTs, respectively [34–36]. To describe the cubic–orthorhombic MT observed in Cu–Al–Ni alloy experimentally, it is convenient to approximate the orthorhombic unit cell by a tetragonal cell with the same volume. The cubic–tetragonal MT is described by the Landau expansion of the Gibbs potential

$$
\begin{aligned}
G(T, t) = {} & \tfrac{1}{2}c_1 u_1^2 + \tfrac{1}{2}c_2(T)(u_2^2 + u_3^2) + \tfrac{1}{2}a_2 u_1(u_2^2 + u_3^2) \\
& + \tfrac{1}{3}a_4 u_3(u_3^2 - 3u_2^2) + \tfrac{1}{4}b_4(u_2^2 + u_3^2)^2 \\
& + \tfrac{1}{2}b_7 u_1 u_3(u_3^2 - 3u_2^2) + 3P^{(i)}(t)u_1 \\
& - \tfrac{1}{6}(\sigma_2^{(i)}(t)u_2 + \sigma_3^{(i)}(t)u_3),
\end{aligned}
\tag{1}
$$

where $u_1 = (\varepsilon_{xx} + \varepsilon_{yy} + \varepsilon_{zz})/3$, the values

$$
u_2 = \sqrt{3}(\varepsilon_{xx} - \varepsilon_{yy}), \qquad u_3 = 2\varepsilon_{zz} - \varepsilon_{yy} - \varepsilon_{xx} \tag{2}
$$

are the components of the two-component order parameter of the cubic–tetragonal MT, where ε_{ik} are the strain tensor components [26], the coefficients $a_{2,4}$, $b_{4,7}$ and $c_{1,2}$ are linear combinations of the second-, third-, and fourth-order elastic moduli [37], and time-dependent values $P^{(i)}(t)$ and $\sigma_{2,3}^{(i)}(t)$ are the isotropic and anisotropic parts of the internal stress arising during the reconfiguration of crystallographic defects after the MT [25].

The minimization of the energy equation (1) enables the description of MTs if the martensitic state obeys the thermoelastic equilibrium principle (see e.g. [7, 8]). As is known [8], the tendency to volume conservation is observed in shape memory alloys, which exhibit thermoelastic equilibrium. In this case the volume change during the MT is small in comparison with the shear strain and can be expressed through the order parameter components using the extremum condition $\partial G/\partial u_1 = 0$, resulting in the equation

$$
\begin{aligned}
\Delta V/V = 3u_1 = {} & -\frac{3a_2}{2c_1}\left(u_2^2 + u_3^2\right) \\
& -\frac{3b_7}{2c_1}u_3\left(u_3^2 - 3u_2^2\right) - \frac{9P^{(i)}}{c_1}.
\end{aligned}
\tag{3}
$$

The first and second terms on the right-hand side of equation (3) express the spontaneous volume change that arises immediately after the MT, and the third term expresses the time-dependent part of the volume change that arises during martensite ageing. The spontaneous volume change is negative for the majority of alloys, because the MTs show a tendency to close packing of atoms. The internal pressure that stabilizes the martensitic phase must make an additional

negative contribution to the volume change. In this case the inequality $P^{(i)} > 0$ holds in the martensitic phase.

If the spatial distribution of the crystal defects possesses the symmetry of the cubic crystal lattice the $P^{(i)}(t)$ and $\sigma_{2,3}^{(i)}(t)$ are equal to zero in the completely relaxed cubic phase, while in the martensitic phase they are expressed as

$$
\begin{aligned}
P^{(i)}(t) &= P^{(i)}(\infty)\left[1 - \exp(-t/\tau_1)\right], \\
\sigma_{2,3}^{(i)}(t) &= \sigma_{2,3}^{(i)}(\infty)\left[1 - \exp(-t/\tau_{2,3})\right],
\end{aligned}
\tag{4}
$$

where $P^{(i)}(\infty)$ and $\sigma_{2,3}^{(i)}(\infty)$ are the saturation pressure and axial stress values, respectively, and the values of τ_1 and $\tau_{2,3}$ are the relaxation times. Equations (4) were obtained in [25, 26] from the expression for the non-scalar 'configurational' order parameter, which describes the adjustment of the spatial configuration of the defect subsystem to the symmetry of the crystal lattice in the martensitic phase. It should be noticed that an equation, similar to equation (4), was obtained previously for the scalar configurational parameter involved in the one-dimensional Landau theory [32].

The appearance of an anisotropic part in the internal stress is stipulated by the SC-SRO principle [21, 23]. Its contribution to the physical effects that accompany martensite ageing are considered in [19, 25]. The isotropic part of the internal stress was considered first in [25, 26] and its role in the martensite stabilization effect was illustrated.

The substitution of the volume change (equation (3)) into equation (1) results in the expression

$$
\begin{aligned}
G^*(T, t) = {} & c_2^*(T, t)(u_2^2 + u_3^2)/2 + a_4^*(t)u_3(u_3^2 - 3u_2^2)/3 \\
& + b_4(u_2^2 + u_3^2)^2/4 - (\sigma_2^{(i)}(t)u_2 + \sigma_3^{(i)}(t)u_3)/6,
\end{aligned}
\tag{5}
$$

where

$$
\begin{aligned}
c_2^*(T, t) &= c_2(T) - 3a_2 P^{(i)}(t)/c_1, \\
a_4^*(t) &= a_4 - 9b_7 P^{(i)}(t)/2c_1,
\end{aligned}
\tag{6}
$$

are the time-dependent energy coefficients, which are renormalized by the internal pressure. The renormalized coefficient of the second-order energy term is related to the shear modulus as $c_2^*(T, t) = C'/3$ [36, 37].

The temperature and time dependences of the MT strain can be obtained by minimization of the potential (5). In the absence of axial stress these dependences are expressed as [36]

$$
\begin{array}{lll}
u_2 = 0, & u_3 = u_0 & \text{in } z\text{-domain}, \\
u_3 = u_2/\sqrt{3} = -u_0/2 & & \text{in } y\text{-domain}, \\
u_3 = -u_2/\sqrt{3} = -u_0/2 & & \text{in } x\text{-domain},
\end{array}
\tag{7}
$$

$$
u_0(T, t) = -\frac{a_4^*(t)}{2b_4}\left(1 + \sqrt{1 - c_2^*(T, t)/c_t^*(t)}\right),
\tag{8}
$$

where $c_t^* = (a_4^*)^2/4b_4$. The austenitic phase is stable if $c_2^*(T, t) > 0$, whereas the martensitic phase is stable for $c_2^*(T, t) < c_t^*(t)$ [36]. The equations $c_2^*(T_{\mathrm{MS}}, t) = c_t^*(t)$ and $c_2^*(T_{\mathrm{MF}}, t) = 0$ prescribe the starting and finishing MT temperatures $T_{\mathrm{MS}}(t)$ and $T_{\mathrm{MF}}(t)$, respectively. It can be seen from equation (8) that $u_0(T_{\mathrm{MF}}, t) = -a_4^*(t)/b_4$.

The thermodynamic system described by the Gibbs potential undergoes a cubic-to-tetragonal transformation in a single crystal form and our experimental results are for a cubic-to-orthorhombic transition in a polycrystal CuAlNi alloy. To enable a direct comparison of the theoretical model with experiment we approximated the orthorhombic unit cell by a tetragonal unit cell with the same volume and adopted the following assumptions:

(i) the single-crystalline grains are separated by low-angle boundaries;
(ii) every grain is internally twinned in the martensitic state and its twin structure is formed by two alternating variants of the tetragonal lattice;
(iii) the *xy*-, *xz*- and *yz*-twins occupy the same fractional volumes (*x*, *y* and *z* denote the directions of the principal crystallographic axes of the twin components).

The orthorhombic unit cell with lattice parameters $a_{\text{exp}} = 0.4382$ nm, $b_{\text{exp}} = 0.5356$ nm and $c_{\text{exp}} = 0.4222$ nm is replaced by a tetragonal cell with the averaged parameters $a = c = (a_{\text{exp}}c_{\text{exp}})^{1/2}$, $b = b_{\text{exp}}$ and correct volume $a^2 b = a_{\text{exp}}b_{\text{exp}}c_{\text{exp}}$ because the relative difference between a and a_{exp} (or c and c_{exp}) is close to 2%, while the relative difference between a_{exp} (or c_{exp}) and b_{exp} is close to 20%.

Three specific assumptions which relate polycrystal properties to single crystal properties are well adopted. Under assumption (i) the crystallographic directions ⟨100⟩ are almost the same all over the crystal; assumption (ii) provides the presence of the coherent interfaces, which determine the specific properties of the martensitic state; according to assumption (iii) the *macroscopic* symmetry of the sample is cubic and the Young's modulus is expressed as $E_M = 2\bar{C}'(\bar{C}_{11} + 2\bar{C}_{12})/(\bar{C}_{11} + \bar{C}_{12})$ in the martensitic phase. The values $\bar{C}_{11}$, $\bar{C}_{12}$ and $\bar{C}' = (\bar{C}_{11} - \bar{C}_{12})/2$ are the *average* elastic moduli of the sample in the martensitic state. It is important that when the average shear modulus $\bar{C}'$ is substantially smaller than the moduli $\bar{C}_{11}$ and $\bar{C}_{12}$, the Young's modulus is approximately equal to $3\bar{C}'$. The expressions for the elastic moduli of the martensitic structure formed by the two alternating variants of the tetragonal lattice were obtained in [36]. Using the results of this work the Young's modulus of twinned martensite can be expressed as

$$E_M(T, t) = \frac{-54u_0(T, t)(a_4^*(t))^2 - 108a_4^*(t)b_4u_0^2(T, t)}{b_4u_0(T, t) - 4a_4^*(t)}. \quad (9)$$

(The volume fractions of the twin components are assumed to be equal to each other, for more details see [36].)

The order parameter is related to the MT strain as $\varepsilon_M(T, t) = u_0(T, t)/3$. Due to this equation (9) enables (i) the determination of the temperature and time dependences of Young's modulus from the experimental value $E_M(T_{\text{MF}}, 0)$ and the experimental temperature dependence of the MT strain; (ii) the determination of the temperature and time dependences of the MT strain from the experimental value $\varepsilon_M(T_{\text{MF}}, 0)$ and the experimental temperature dependence of Young's modulus. The solution to problem (i) is presented in [38] for two Ni–Mn–Ga single crystals with substantially

different MT temperatures. The solution of problem (ii) is presented below for the polycrystalline Cu–13.8Al–4.0Ni alloy specimen. The solution of the problem involves three steps.

First, the value $E_M(T, 0)$ must be determined from the experimental temperature dependence of the storage modulus (see figure 2).

Second, the values $a_4^*(0)$, b_4 must be found from the equations

$$a_4^*(0) = -E_M(T_{\text{MF}}, 0)/10.8u_0(T_{\text{MF}}, 0),$$
$$b_4 = E_M(T_{\text{MF}}, 0)/10.8u_0^2(T_{\text{MF}}, 0), \quad (10)$$

which were obtained by substituting the value $u_0(T_{\text{MF}}, 0) = -a_4^*(0)/b_4$ into equation (9).

Third, the temperature and time dependences of the MT strain can be recovered from the experimental temperature dependence of the storage modulus and equation (9). The temperature dependence of the MT strain follows from the experimental temperature dependence of the elastic modulus, while its time dependence results from equations (4), (6) and (9).

The Young's modulus of the austenitic phase is related to the shear modulus of the cubic lattice and the coefficient of the Landau expansion as

$$E_A(T, t) = 3C' = 9c_2^*(T, t). \quad (11)$$

Both experiment and theory demonstrate that not only the internal axial stress but also the internal pressure can contribute to the martensite ageing effects. The symmetry-conforming internal stress does not reduce the tetragonal symmetry of martensitic domains; therefore, the equalities $u_2 = 0$, $u_3 = u_0$ and equations (7), (9), (10) hold true even *in the presence of axial stress*. At the same time, equation (8), which was obtained for the unstressed crystal, must be replaced by the equation

$$c_2^*(T, t)u_0 + a_4^*(t)u_0^2 + b_4u_0^3 - \sigma_3^{(i)}(t)/6 = 0, \quad (12)$$

which expresses the extremum condition $\partial G^*/\partial u_3 = 0$ for the Gibbs potential equation (5) of the axially stressed crystal. Equation (12) enables the calculation of the time- and temperature-dependent values of the order parameter u_0.

Equations (4), (6) and (8)–(12) form the basis for the theoretical modeling of ageing effects on the Young's modulus.

4. Computations

In this section, we utilize equations (4), (6), (8)–(12) to quantitatively describe the time and temperature dependences of the MT strain and storage modulus of martensitic alloy during ageing. To this end, one must know the values of the MT temperatures, volume change during MT, $u_0(T_{\text{MF}}, 0)$ and the temperature dependence of the storage modulus. As can be seen from figure 1(a), the values $T_{\text{MS}} \approx 405$ K and $T_{\text{MF}} \approx 375$ K can be accepted for the Cu–13.8Al–4.0Ni alloy. The orthorhombic unit cell of the martensitic phase
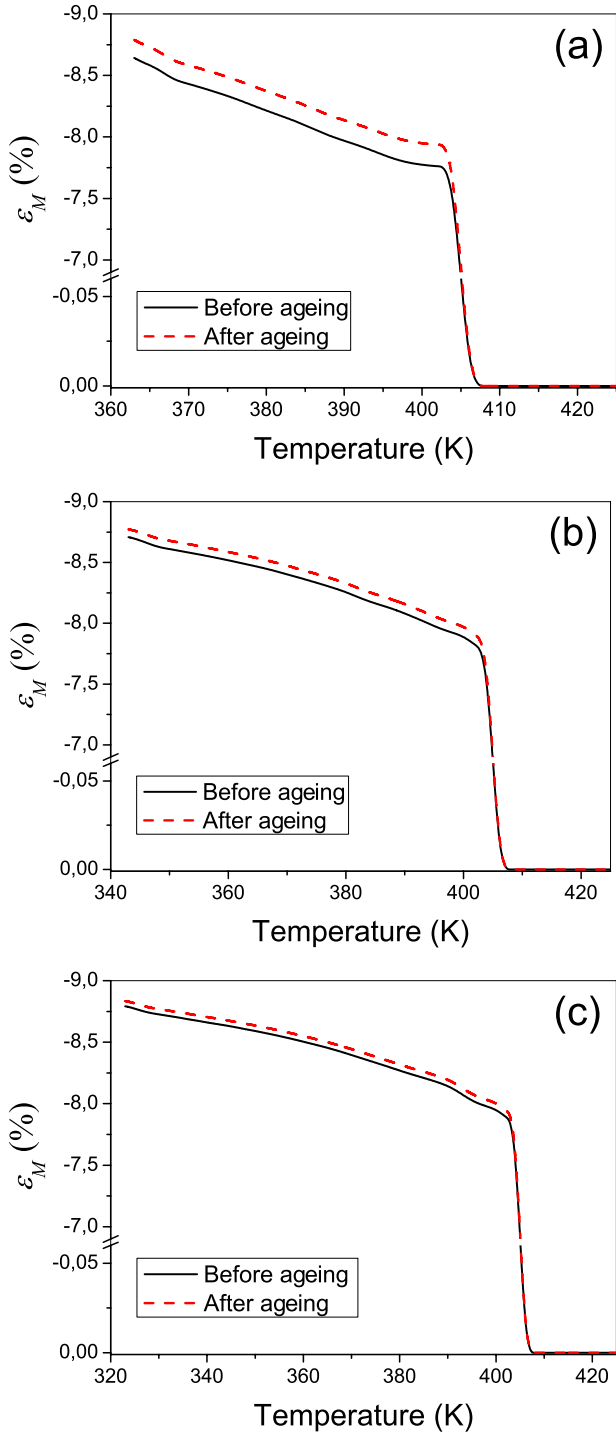
Table 1. Characteristic times of the internal pressure and axial stress variation.

T (K)	363	343	323
τ_1 (min)	18	45	70
τ_3 (min)	180	1050	3000

in a volume change during MT

$$\frac{\Delta V}{V} = \frac{2a_{exp}b_{exp}c_{exp} - a_0^3}{a_0^3} = \frac{2a^2b - a_0^3}{a_0^3} \approx -3 \times 10^{-3} \quad (13)$$

and the order parameter value $u_0(T_{MF}, 0) = 3\varepsilon_M(T_{MF}, 0) = -0.25$. These input data enable the evaluation of the coefficients involved in equations (5), (6) and (12), seen in [37, 38].

The MT strains $\varepsilon_M(T, t)$ computed from equation (12) for ageing times $t = 0$ and 360 min are shown in figure 4 as solid and dashed lines, respectively.

The results presented in figure 4 prove that it is possible to reconstruct the temperature dependence of the MT strain from the temperature dependence of Young's modulus measured for the spatially inhomogeneous martensitic state. So, the temperature dependence of the MT strain of the *aged* martensite was reconstructed from the experimental temperature dependence of the storage modulus of *fresh* martensite. To illustrate the accuracy of the theoretical evaluation of the energy coefficients and MT strain, the inverse problem was resolved, that is, the Young's modulus was computed from equations (9)–(11) using the $\varepsilon_M(T)$ functions shown in figure 4. The obtained results are presented in figure 2 as solid lines. The excellent fit of the lines to experimental points illustrates only the high accuracy of the previously computed $\varepsilon_M(T)$ values. However, the resolution of the inverse problem is of significance in its own right, because it shows that the temperature dependence of the Young's modulus can be determined if the temperature dependences of lattice parameters are known.

The theoretical time dependence of Young's modulus of Cu–13.8Al–4.0Ni alloy is shown in figure 3. The lines in figure 3 are computed for three constant temperatures under the assumption that the ageing is accompanied by two physical processes: one is characterized by the internal pressure $P^{(i)}(\infty) = 0.4$ GPa and the other is characterized by the internal axial stress $\sigma_3^{(i)}(\infty) = 2\sigma_{zz}^{(i)}(\infty) = -27$ MPa. These values and the characteristic times of these processes were determined by fitting the theoretical time dependences of the storage modulus to experimental ones (see figure 3 and table 1). It should be noted that these dependences cannot be determined from the one-dimensional theories [31–33], because each of these theories involves only one slowly variable parameter that characterizes the defect reconfiguration/relaxation.

Table 1 demonstrates the dependence of the characteristic times on the ageing temperature reported by many authors (see [15, 16, 19] and references therein). Table 1 also shows that the isotropic component of internal stress rises substantially quicker than the anisotropic one. This feature of

Figure 4. Theoretical dependences of the martensitic transformation strain computed for fresh (solid lines) and aged (dashed lines) martensite. Computations were carried out using the experimental temperature dependences of the storage modulus of the alloy aged at 363 (a), 343 (b) and 323 K (c).

was approximated by a tetragonal cell with the same volume. The lattice parameters of the tetragonal unit cell $b = b_{exp} = 0.5356$ nm, $a = c = (a_{exp}c_{exp})^{1/2} = 0.4301$ nm were calculated using the experimental values of the lattice parameters reported for the orthorhombic phase of the Cu–14.2Al–4.3Ni alloy [39]. These lattice parameters result

the martensite stabilization process can be explained by the noticeable difference in the values of the bulk elastic modulus and the shear elastic modulus of shape memory alloys. Indeed, the martensitic transformation is accompanied by both a volume change and a shear deformation of the crystal lattice. The defects slow the achievement of the optimal volume and shape of the crystal. As such the energy difference between the optimal and instant states of the lattice with defects arises immediately after the martensitic transformation. Due to the large value of the bulk elastic modulus, the deviation from the optimal volume induces large elastic forces acting on defects. Therefore, the characteristic time of the approach to the equilibrium volume value is small. The shear modulus is smaller by an order of magnitude than the bulk modulus; thus, the elastic forces which cause the defect reconfiguration are also small and need more time for a crystal with defects to approach the equilibrium shape.

5. Discussion and conclusions

In the present study, *in situ* DMA measurements were carried out to obtain the temperature and time dependences of the storage modulus of Cu–Al–Ni shape memory alloy. The theoretical analysis showed that the experimentally observed gradual increase of storage modulus during martensite ageing cannot be described solely by the time-dependent axial stress (as it is seen in figure 5(a)). A quantitative theoretical treatment of experimental data further shows that the experimental time dependence of the storage modulus can be satisfactorily described using two exponential functions with different exponents. The first function describes the time dependence of the axial internal stress, which is explicitly present in equation (12) and used for the computation of Young's modulus. Distinct from this, the second function describes the time dependence of the internal pressure and implicitly affects the time dependence of Young's modulus through the renormalization of the energy coefficients (equation (6)) involved in equation (12). The time-dependent axial stress responds to the symmetry breakdown caused by the MT while the internal pressure responds to the volume change during the MT. As shown in figure 5(b), these two mechanisms of defect reconfiguration contribute noticeably to the time dependence of the storage modulus. The combination of the two mechanisms of defect reconfiguration with different rates gives rise to the accurate time-dependent behavior of the alloy (see figure 3).

Comparing the contributions of isotropic internal pressure and axial stress to the time dependence of Young's modulus (figure 5(b)) we can verify the idea concerning the influence of the volume change during MT on the elastic properties of the shape memory alloy. To this end, the product of the bulk elastic modulus and the volume change should be compared with the product of the storage modulus and the MT strain, because these products characterize the energy changes estimated in section 1. For the Cu–14Al–4.1Ni alloy studied in [40] the bulk modulus is $B \approx 130$ GPa. The values $E = 14$ GPa (figure 2), $\Delta V/V = -3 \times 10^{-3}$ (equation (13)) and $\varepsilon_M = -0.085$ (figure 4) result in the energy changes
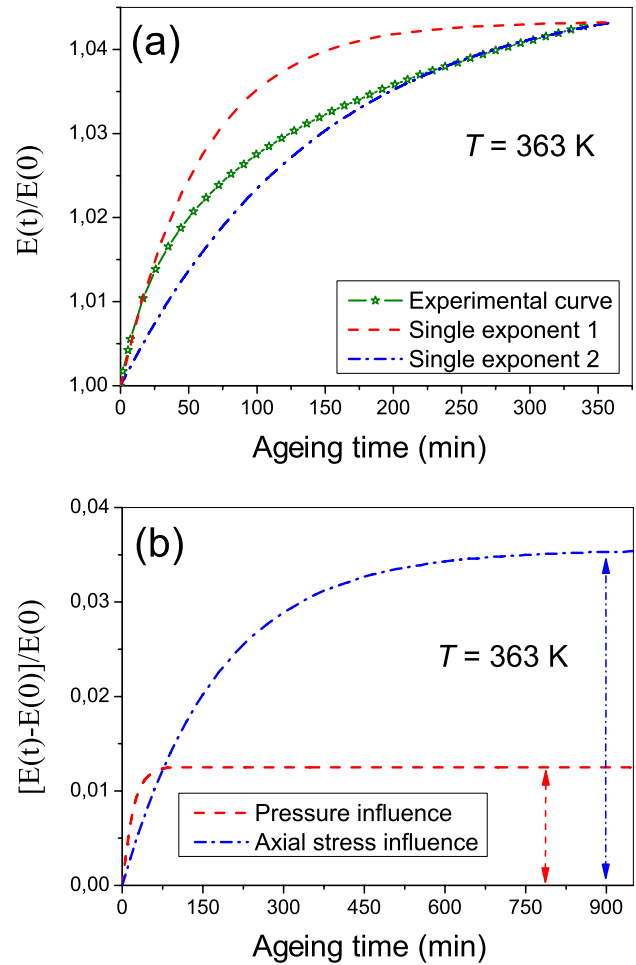

Figure 5. Exponential fits to the initial and final fragments of the experimental time dependence of the storage modulus, (a). The contributions of isotropic internal pressure and axial stress to the time dependence of Young's modulus are shown in (b).

$(\Delta V/V)B \approx -0.39$ GPa and $E\varepsilon_M \approx -1.19$ GPa. The ratio of these values is approximately equal to 0.33. Figure 5(b) shows that the ratio of values $[E(900) - E(0)]/E(0)$ caused by the isotropic internal pressure and axial internal stress (see two-sided arrows) is approximately equal to 0.35. The proximity of the two estimated ratios suggests that the time variation of the storage modulus is controlled by the elastic energy differences between the instant and optimal states of the crystal lattice with defects. It opens up a prospect for evaluating internal stresses by means of first-principles calculations (see [41] and references therein).

From the above analysis, it can be seen that the symmetry-conforming Landau theory does not fully agree with the basic points of the SC-SRO principle [21, 22]. The latter relates the reconfiguration of the defect subsystem and the concomitant physical effects only to the symmetry change caused by the MT. Here, our computation on the experimental results shows that the energy of the defect subsystem depends on the volume of the alloy specimen as well. Therefore, both symmetry and volume changes during MT provoke the defect reconfiguration.

It should also be noticed that the knowledge of the experimental temperature dependence of Young's modulus of the spatially inhomogeneous martensitic state enables the evaluation of the coefficients of the symmetry-conforming Landau expansion for the Gibbs potential. Due to this, the symmetry-conforming Landau theory can be used for a quantitative description of the temperature/time dependences of the storage modulus, martensitic transformation strains and relevant properties of shape memory alloys.

Acknowledgments

References

[1] Pálsson G K, Wälde M, Amft M, Wu Y, Ahlberg M, Wolff M, Pundt A and Hjörvarsson B 2012 *Phys. Rev.* B **85** 195407
[2] Jiles D C 2003 *Acta Mater.* **51** 5907
[3] Murray S J, Marioni M, Allen S M, O'Handley R C and Lograsso T A 2000 *Appl. Phys. Lett.* **77** 886
[4] Likhachev A A, Sozinov A and Ullakko K 2004 *Mater. Sci. Eng.* A **378** 513
[5] Nix W D, Gibeling J C and Hughes D A 1985 *Metall. Trans.* A **16** 2215
[6] Hardy V, Maignan A, Hébert S, Yaicle C, Martin C, Hervieu M, Lees M R, Rowlands G, Paul D Mc K and Raveau B 2003 *Phys. Rev.* B **68** 220402
[7] Wayman C M 1964 *Introduction to the Crystallography of Martensitic Transformations* (New York: MacMillan)
[8] Warlimont H and Delaey L 1974 *Martensitic Transformations in Copper- Silver- and Gold-based Alloys* (Oxford: Pergamon)
[9] Ölander A 1932 *J. Am. Chem. Soc.* **54** 3819
[10] Miura S, Maeda S and Nakanishi N 1974 *Phil. Mag.* **30** 565
[11] Sakamoto H, Otsuka K and Shimizu K 1977 *Scr. Metall.* **11** 607

[12] Barceló G, Rapacioli R and Ahlers M 1978 *Scr. Metall.* **12** 1069
[13] Arab A A and Ahlers M 1988 *Acta Metall.* **36** 2627
[14] Murakami Y, Nakajima Y, Otsuka K, Ohba T, Matsuo R and Ohshima K 1997 *Mater. Sci. Eng.* A **237** 87
[15] Santamarta R, Seguì C, Pons J and Cesari E 1999 *Scr. Mater.* **41** 867
[16] Seguì C, Cesari E, Font J, Muntasell J and Chernenko V A 2005 *Scr. Mater.* **53** 315
[17] Saule F and Ahlers M 1995 *Acta Metall. Mater.* **43** 2373
[18] Picornell C, Pons J, Cesari E, Chumlyakov Y I and Dutkiewicz J 2009 *Funct. Mater. Lett.* **2** 83
[19] Xue D, Zhou Y, Ding X, Otsuka K, Sun J and Ren X 2011 *Acta Mater.* **59** 4999
[20] Marukawa K and Tsuchiya K 1995 *Scr. Metall.* **32** 77
[21] Ren X and Otsuka K 1997 *Nature* **389** 579
[22] Ren X and Otsuka K 2000 *Phys. Rev. Lett.* **85** 1016
[23] Otsuka K and Ren X 2001 *Mater. Sci. Eng.* A **312** 207
[24] Ishibashi K *et al* 2002 *Mater. Sci. Eng.* A **329–331** 568
[25] L'vov V A, Kosogor A, Söderberg O and Hannula S-P 2010 *Mater. Sci. Forum* **635** 13
[26] Kosogor A, L'vov V A, Söderberg O and Hannula S-P 2011 *Acta Mater.* **59** 3593
[27] Gefen Y, Halwany A and Rosen M 1973 *Phil. Mag.* **28** 1
[28] Kakeshita T, Yoshimura Y, Shimizu K, Endo S, Akahama Y and Fujita F E 1988 *Trans. Japan Inst. Metals* **29** 781
[29] Buchelnikov V D, Khovailo V V and Takagi T 2006 *J. Magn. Magn. Mater.* **300** e459
[30] L'vov V A, Kosogor A, Barandiaran J M and Chernenko V A 2012 *Acta Mater.* **60** 1587
[31] Bhattacharya K, James R D and Swart P J 1997 *Acta Mater.* **45** 4547
Bhattacharya K, James R D and Swart P J 1997 *Acta Mater.* **45** 4561
[32] Ohta T 2001 *Mater. Sci. Eng.* A **312** 57
[33] Okuzono T, Yamazaki Y and Ohta T 2003 *Phys. Rev.* B **67** 054106
[34] Liakos J K and Saunders G A 1982 *Phil. Mag.* A **46** 217
[35] Barsch G R and Krumhansl J A 1984 *Phys. Rev. Lett.* **53** 1069
[36] Gomonaj E V and L'vov V A 1996 *Phase Trans.* **56** 43
[37] Chernenko V A and L'vov V A 1996 *Phil. Mag.* A **73** 999
[38] L'vov V A, Glavatska N, Aaltio I, Söderberg O, Glavatskyy I and Hannula S-P 2009 *Acta Mater.* **57** 5605
[39] Otsuka K and Shimizu K 1974 *Trans. Japan Inst. Metals* **15** 103
[40] Sedlák P, Seiner H, Landa M, Novák V, Šittner P and Mañosa L I 2005 *Acta Mater.* **53** 3643
[41] Gruner M E and Entel P 2011 *Phys. Rev.* B **83** 214415